Effects of magnetic transitions on the optical energy gap values of some $I_2.Mn.IV.VI_4$ phases

1993 J. Phys.: Condens. Matter 5 7143

(http://iopscience.iop.org/0953-8984/5/38/010)

J. Phys.: Condens. Matter 5 (1993) 7143–7154. Printed in the UK

Effects of magnetic transitions on the optical energy gap values of some I_2.Mn.IV.VI_4 phases

X L Chen, A-M Lamarche, G Lamarche and J C Woolley

Ottawa–Carleton Institute for Physics, University of Ottawa, Ottawa, Ontario, Canada K1N 6N5

Received 16 February 1993, in final form 25 May 1993

Abstract. Optical absorption measurements were made to determine optical energy gap values as a function of temperature on samples of Cu_2MnGeS_4, $Cu_2MnSiSe_4$ (both antiferromagnetic), $Ag_2MnGeSe_4$ and $Ag_2MnSiTe_4$ (both ferrimagnetic) with the orthorhombic structure, and of $Ag_2MnSiTe_4$ with the cubic structure (ferrimagnetic). These data were analysed to determine the contribution ΔE to the energy gap due to magnetic effects in the temperature region around the critical temperature T_N. It was shown that the magnetic contribution increased the energy gap for the antiferromagnetic cases and decreased the energy gap for the ferrimagnetic ones. The variation of ΔE with T was found to agree very well with the theoretical predictions of Alexander *et al.*

1. Introduction

Magnetic semiconductors and alloys in which manganese is one of the component elements are of interest because of the large magneto-optical effects which can occur in these materials. Most work has so far been concerned with the semimagnetic semiconductor alloys obtained from the II.VI compounds by replacing a fraction of the group-II cations with Mn, producing an alloy which shows spin-glass behaviour [1]. It was recently suggested [2–4] that larger magneto-optical effects than those for the II.VI-derived alloys could be obtained in materials in which the antiferromagnetic interaction between nearest-neighbour Mn ions was smaller, and the interaction between ions on the same magnetic sublattice was greater. It was suggested that one set of materials which could satisfy these conditions were the I_2.Mn.IV.VI_4 compounds.

The initial work on such compounds with I=Cu and VI=S or Se [5–9] indicated that they showed either the tetragonal stannite or the orthorhombic wurtz–stannite structure. However, recent work in the present programme [10] has shown that many of the Ag and Se or Te compunds can show two different structures depending upon the heat treatment used in their preparation. While all compounds show either the tetragonal or orthorhombic structure as one form, the second structure shown in each case appears to be cubic, with the main x-ray diffraction lines corresponding to the rock-salt structure, but with faint ordering lines observed in most cases. It was also found that all of the Te compounds are unstable at lower temperatures ($\leqslant 400\,^{\circ}C$), giving two or more phases, one of which is $MnTe_2$. However, it was found that if a single-phase sample was rapidly quenched from the higher temperature, the phase was metastable at room temperature, the samples showing the same crystallographic and magnetic behaviour for up to two years after production as observed in the initial measurements.

0953-8984/93/387143+12$07.50

Measurements of magnetic susceptibility as a function of temperature [11] showed that many of the Se and Te phases were ferrimagnetic with Néel temperatures lying in the range 50–250 K. The analysis of the crystallographic and magnetic parameters [10, 11] suggested that different phases showed different ordered structures, although these have not as yet been determined. For this reason, the phases are referred to here as orthorhombic, tetragonal and cubic, although it is probable that some of the ordered structures have lower symmetry.

One semiconductor property which is affected by the magnetic behaviour of these materials containing Mn is the band gap. Theoretical analysis by Alexander *et al* [12] of the effects of spin fluctuations around a magnetic critical point on the energy value of band extrema has shown that around such a critical point, in addition to the normal semiconductor effects, there will be a magnetic contribution to the variation of the band gap with temperature. They indicated that for an antiferromagnetic exchange interaction, the effect should cause an increase in the band gap of the semiconductor, while a decrease in band gap should be observed for a ferromagnetic exchange. In a range of II.VI and I.III.VI_2 based alloys involving Mn (e.g. $Cd_{1-z}Mn_zTe$, $(CuIn)_{1-z}Mn_{2z}Te_2$), the exchange interaction is antiferromagnetic and it has been shown for a number of cases [13–15] that the variation of band gap with temperature in these materials is in good agreement with the predictions of Alexander *et al*. In recent work, a similar investigation was reported for the orthorhombic phase of the compond $Ag_2MnGeSe_4$ [16], which shows ferrimagnetic behaviour [11]. In this case, it was found that the optical energy gap was reduced in the vicinity of the magnetic critical temperature and that again the variation with temperature was consistent with the predictions of the theoretical analysis [12]. In the present work, measurements have been made as a function of temperature of the optical energy gap values of four different I_2.Mn.IV.VI_4 phases, i.e. the orthorhombic phases of Cu_2MnGeS_4, $Cu_2MnSiSe_4$ and $Ag_2MnSiTe_4$ and the cubic phase of $Ag_2MnSiTe_4$. (For convenience, these will be labelled CuGeS (o) and AgSiTe (c) etc in the following text.) The resulting data for these cases were analysed, and the previous data for AgGeSe (o) re-analysed, in terms of the model of Alexander *et al*.

2. Sample preparation and experimental measurements

All of the samples were prepared as indicated in the previous crystallographic work [10]. Thus, in each case, the component elements were sealed under vacuum in a quartz capsule, which had previously been internally coated with carbon to prevent reaction of the charge with the quartz. The samples were then heated to 1150 °C, in the case of the Se and Te compounds in approximately an hour, but at a much slower rate for the sulphide with stops at intermediate temperatures to allow reaction to occur. The samples were held at 1150 °C for $\frac{1}{2}$–1 hour and then cooled to room temperature. The samples were then annealed at the appropriate temperature to produce the phase required, and were finally quenched to room temperature in a brine solution. In each case, a Debye–Scherrer x-ray powder photograph was taken of the resulting sample, to check that the required phase was obtained. In the case of the telluride compound (AgSiTe), since the equilibrium condition at room temperature is multiphase, even for rapidly quenched samples some traces of other phases may occur, and care was taken to keep these effects to a minimum in the samples investigated. As discussed in the magnetic work [11], it is also possible in some cases to obtain a mixture of both phases of the compound in the chosen sample. This problem was not important in the present work since CuGeS (o), CuSiSe (o) and AgGeSe (o) are the only structures which occur for each of these compounds. In the case of AgSiTe, previous work had shown that it

was almost impossible with the techniques used here to obtain a single-phase sample of the cubic structure, and so the optical sample was prepared so as to give the orthorhombic phase. However, it was found that a small percentage of the cubic phase was always present, and when the optical measurements were analysed, this was found to be a useful condition since the values of the energy gaps of the two different phases could be separately determined from the one set of data.

Values of the optical energy gap E_0 were determined by the optical absorption method described previously [17]. A slice cut from the sample ingot was polished down to a thickness d in the range $50 < d < 100$ μm and used for standard transmission measurements. The variations of I_0, the incident intensity, and I, the transmitted intensity, as a function of photon energy $h\nu$ were determined separately as continuous curves on a chart recorder, and hence values were calculated for the ratio I_0/I (in arbitrary units) as a function of $h\nu$. The resulting values of $\ln(I_0/I)$ thus had an arbitrary zero and also a background value due to various scattering effects in the sample, as seen in figures 1, 5 and 9. The $\ln(I_0/I)$ values were therefore corrected by subtracting an effective constant background value, independent of $h\nu$, so as to give values proportional to the absorption coefficient α. The case for the AgSiTe sample was a little more complicated and is discussed further below. In all cases, a graph of $(\alpha h\nu)^2$ versus $h\nu$ was plotted and for all except CuSiSe (o) the graph showed good linear form, indicating a direct gap. The case of CuSiSe (o) will be discussed in more detail below.

The optical samples were mounted in a Cryodine 215C cryocooler so that the temperature could be controlled at any point in the range 10–300 K. For each case investigated, values of E_0 were determined at about 15 temperatures in the available range to show the variation of E_0 with T. The analysis of these data is discussed in detail below.

3. Results and analysis

3.1. CuGeS (o)

CuGeS shows only the orthorhombic structure [10] and is antiferromagnetic with $T_N = 10$ K [11]. The experimentally determined variation of $\ln(I_0/I)$ with $h\nu$ at 200 K and the corresponding graph of $(\alpha h\nu)^2$ versus $h\nu$ are shown in figure 1(*a*) and (*b*) respectively. In figure 1(*b*), a straight line can be drawn as shown through the points above the tail, giving a value of E_0 of 2.035 eV. Similar measurements at other temperatures gave corresponding E_0 values, and the variation of E_0 with T is shown in figure 2, the relative error in E_0 being estimated as ± 0.003 eV. The form of this curve shows that E_0 increases slowly as the temperature is reduced from 300 K down to $\sim$ 110 K, consistent with the behaviour of normal semiconductors, but increases more rapidly at lower temperatures, peaking at around 10 K, the Néel temperature of the material. This is consistent with the predictions of Alexander *et al* [12] and with previously observed behaviour for materials having antiferromagnetic exchange [13–15].

The predictions of Alexander *et al* indicate that the variation of the magnetic contribution ΔE to the band gap satisfies a relation of the form

$$(\mathrm{d}/\mathrm{d}t)\Delta E = -Pt^{-\mu} \tag{1}$$

where t is the reduced temperature difference $|T - T_c|/T_c$ and the critical exponent μ depends upon the particular conditions being considered. Integration of (1) gives

$$\Delta E = -Pt^{1-\mu}/(1-\mu) + K. \tag{2}$$

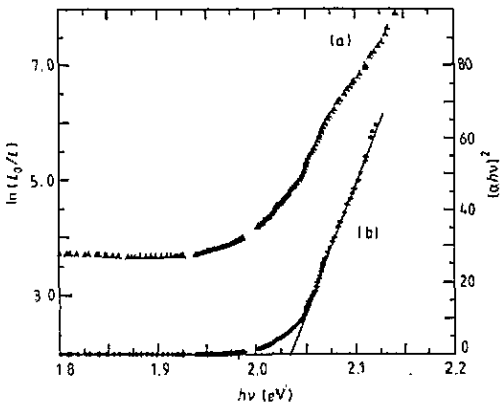

Figure 1. CuGeS (o): variation of (*a*) $\ln(I_0/I)$ and (*b*) $(\alpha h\nu)^2$ with photon energy $h\nu$ at 200 K.

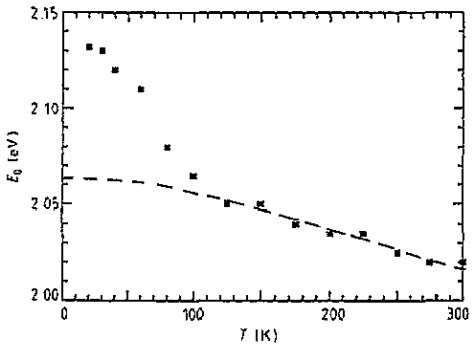

Figure 2. CuGeS (o): variation of optical energy gap E_0 with temperature T. ■, experimental values; – – –, E_{on} values from fit to Manoogian–Leclerc equation.

If the value of ΔE at T_c is written as ΔE_c, the constant of integration can be eliminated and hence

$$\Delta E = -Pt^{1-\mu}/(1-\mu) + \Delta E_c. \tag{3}$$

Thus if values of ΔE are determined from the experimental data, these can be analysed in terms of (3). As indicated previously [13–16], in order to determine ΔE values, it is necessary to know $E_{on}(T)$, the values that the energy gap would have in the absence of any magnetic effects. These can be determined by extrapolating to low temperatures the higher-temperature regions of the E_0 versus T curve, where the magnetic contributions are negligible, i.e. where $E_{on} = E_0$. This may be done using a simple Manoogian–Leclerc equation [18] of the form

$$E_{on}(0) - E_{on}(T) = UT^{2/3} + V\Phi[\coth(\Phi/2T) - 1] \tag{4}$$

where U, V and Φ are constant, independent of temperature.

Thus the data shown in figure 2 have to be fitted to (4) in the temperature range where the magnetic contribution is negligible. There are four parameters in (4) to be determined, viz. E_{on}, V, U and Φ. However, from previous analyses of this type [13–15, 19], it is found that reasonable estimates can be made for some of these, so that the number of parameters to be determined from the data can be conveniently reduced. From the previous work and from the analysis of the data for AgSiTe discussed below, a reasonable estimate for Φ in this case is 220 K. Also, as shown previously [18, 13, 14], the contribution of the U term is smaller than that of the V term, and a good fit to the data can be obtained assuming that $2|U| = |V|$. Thus (4) reduces to

$$E_{on}(0) - E_{on}(T) = (V/2)\{T^{2/3} + 440[\coth(110/T) - 1]\} \tag{5}$$

where for convenience the RHS can be written as $(V/2)X$. Using the experimental E_0 versus T data in the range 125 K $< T <$ 300 K, a linear graph of E_0 versus X is obtained as shown in figure 3, with slope and intercept values giving $V/2 = 5.050 \times 10^{-5}$ eV K^{-1}

and $E_{on}(0) = 2.064$ eV. The resulting curve of E_{on} versus T over the whole range of T is shown in figure 2. Taking $\Delta E = E_0 - E_{on}$, it is seen that ΔE is positive in this case, and from (3), P is also positive. (3) can be written as

$$\ln(\Delta E_c - \Delta E) = \ln[P/(1-\mu)] + \ln t \tag{6}$$

and by extrapolation of the curve drawn through the experimental points, ΔE_c has a value of 0.073 eV. Figure 4 shows the experimental graph of $\ln(\Delta E_c - \Delta E)$ versus $\ln t$, which is seen to be a reasonable straight line, with the experimental scatter being attributed to errors in E_0 and T of approximately equal amounts. The slope and intercept values from figure 4 give $\mu = -0.54$ and $P = +4.6$ meV.

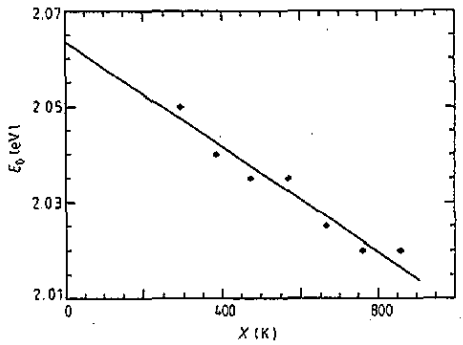

Figure 3. CuGeS (o): variation of optical energy gap E_0 with $X\ (= T^{2/3} + 2\Phi[\coth(\Phi/2T) - 1])$.

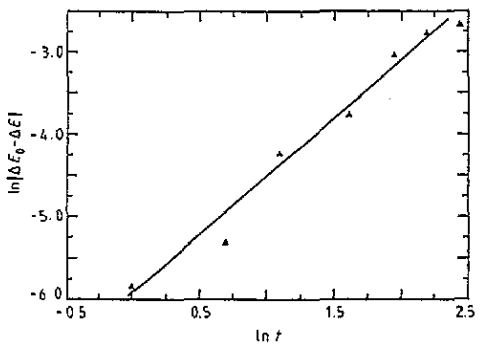

Figure 4. CuGeS (o): variation of $\ln|\Delta E_c - \Delta E|$ with $\ln t$.

3.2. AgSiTe (o+c)

As mentioned above, it was not possible in the present work to obtain a single-phase sample of the cubic structure of AgSiTe, and the preparation of the present sample was arranged to give the orthorhombic phase. However, the x-ray photograph showed a small amount of the cubic phase to be present and, as discussed below, the optical data confirmed this. Previous work [11] had shown that both of these phases are ferrimagnetic, the magnetic susceptibility data indicating that $T_N = 85$ K for the orthorhombic phase and $T_N = 150$ K for the cubic phase. A typical curve showing the variation of $\ln(I_0/I)$ with $h\nu$ for the present sample at 225 K is shown in figure 5. It is seen that there is a rather abrupt change of slope at $h\nu \simeq 1.45$ eV, where the contribution of the main phase begins to dominate, the slope at lower values of $h\nu$ being the contribution of the phase of low concentration. Since if the major phase had the lower band gap the effect of the minor phase would not be observed, it is clear from the x-ray data that the lower-energy gap is that of the cubic phase and the higher gap that of the orthorhombic phase.

Thus when, as indicated above, a background value of $\ln(I_0/I)$ is subtracted, a value of the absorption factor α is obtained which at lower $h\nu$ corresponds to the cubic phase only. The corresponding graph of $(\alpha h\nu)^2$ versus $h\nu$ is also shown in figure 5. It shows reasonable linear form above a low-energy tail as indicated by the straight line on the graph, confirming that the band gap is direct, and extrapolation of this linear part to $(\alpha h\nu)^2 = 0$

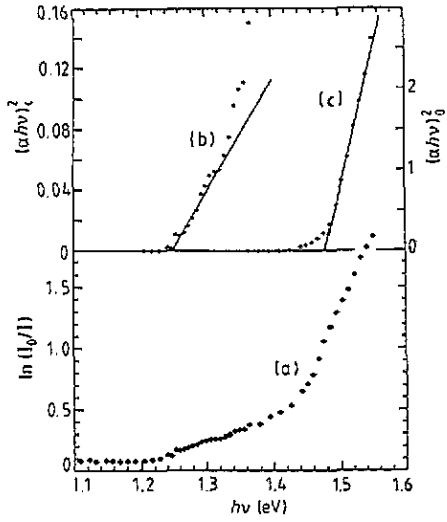

Figure 5. AgSiTe (o+c): variation of (*a*) $\ln(I_0/I)$ and (*b*) $(\alpha h\nu)^2$ for the cubic phase and (*c*) $(\alpha h\nu)^2$ for the orthorhombic phase with photon energy $h\nu$ at 225 K.

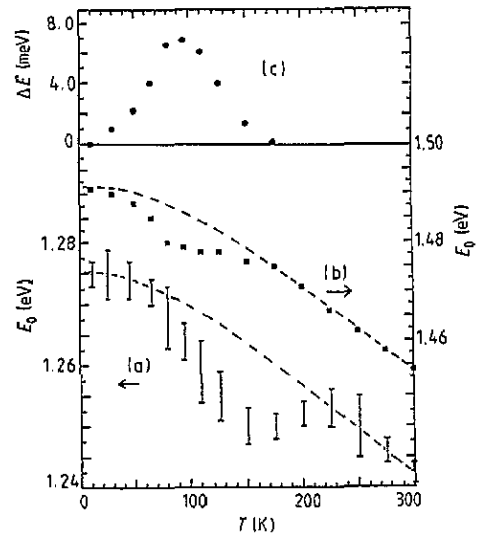

Figure 6. AgSiTe (o+c): (*a*) variation of optical energy gap E_0 for the cubic phase with temperature T. I, experimental values; – – –, E_{on} values from fit to Manoogian–Leclerc equation. (*b*) Variation of the optical energy gap E_0 for the orthorhombic phase with temperature T. ■, experimental values; – – –, E_{on} values from fit to Manoogian–Leclerc equation. (*c*) Variation with temperature T of ΔE, the magnetic contribution to the energy gap, for the orthorhombic phase.

gives an energy-gap value of 1.253 eV for the temperature of 225 K. However, at $h\nu$ values in the vicinity of 1.35 eV, the curve deviates from linear behaviour, showing an increase in absorption due to the band gap of the orthorhombic phase. In this range, the absorption α is the sum of two components, α_c of the cubic phase and α_0 of the orthorhombic phase. By extrapolating the $(\alpha_c h\nu)^2$ line in figure 5, values of α_c were determined for the higher values of $h\nu$, and subtraction from the experimental values of α gave values of α_0. Hence, a graph of $(\alpha_0 h\nu)^2$ versus $h\nu$ was plotted as shown in figure 5. This again shows linear form above a low-energy tail, and extrapolation in this case gives an energy-gap value of 1.466 eV for the temperature of 225 K. Equivalent measurements and analyses were made at other temperatures in the range 10–300 K, and the variations of the band gap E_0 for the two phases are shown in figure 6. For the cubic case, the estimated error varied from temperature to temperature and the data are shown in figure 6 in terms of error bars. For the orthorhombic case, less scatter occurred in the data and the relative error in the points was estimated to be ± 0.003 eV.

Considering first the orthorhombic data (figure 6), the magnetic results indicated that T_N was 85 K and so to fit to the Manoogian–Leclerc form of (4), the data in the temperature range 175–300 K can be used. However, in addition, the value of $E_{on}(0)$ should be very close to the experimental value of E_0 at 10 K, i.e. 1.491 eV, so that this value can be taken as known in the fitting. Thus, if it is again assumed that $2|U| = |V|$, values of V and Φ can be determined from the fit. (4) can be written as

$$E_{on}(0) - E_{on}(T) = (V/2)\{T^{2/3} + 2\Phi[\coth(\Phi/2T) - 1]\} = (V/2)X. \qquad (7)$$

For various trial values of Φ, values of X were calculated and the resulting graphs of $E_{on}(T)$ are shown in figure 7. It is seen that while each value of Φ gives a straight line, the required value of $E_{on}(0) = 1.491$ eV is given only by the line for which $\Phi = 220$ K, confirming that this is the value of Φ to be used with these materials. From the slope of this line, it is found that $V/2 = 4.325 \times 10^{-5}$ eV K^{-1}. Hence, the fitted curve of E_{on} versus T is shown in figure 6. Again, values of $\Delta E(= E_0 - E_{on})$ can be determined, in this case being negative, and the variation of $|\Delta E|$ with T is shown in figure 6. It is seen that the maximum in $|\Delta E|$ occurs at 93 K, with a value of 7.2 meV. When a graph of $\ln|\Delta E_c - \Delta E|$ versus lnt for this case is plotted, if a value of $T_N = 85$ K is used, corresponding to the magnetic data, it is found that the two sections corresponding to the points above and below T_N do not coincide but show two parallel lines. However, if a value of 93 K is used, a good single straight line is obtained, as shown in figure 8. From the slope and intercept of this line, values of $\mu = -0.52$ and $P = -23$ meV are obtained. The difference in the observed values of T_N for the optical and magnetic data could possibly be due to differences in the temperature reading in the two cases, since, particularly in the optical case, the measuring thermocouple cannot be located exactly at the sample position.

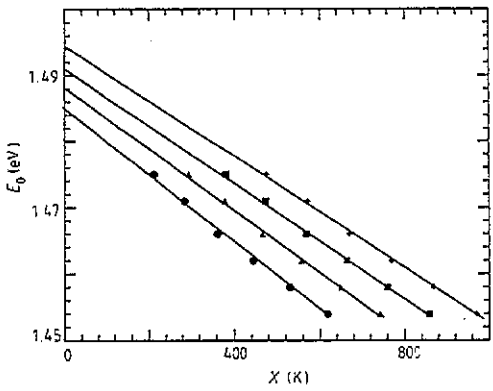

Figure 7. AgSiTe (o): variation of optical energy gap E_0 with $X(= T^{2/3} + 2\Phi[\coth(\Phi/2T) - 1])$ for various values of Φ. Values of Φ: ♦, 150 K; ■, 220 K; ▲, 300 K; ●, 400 K.

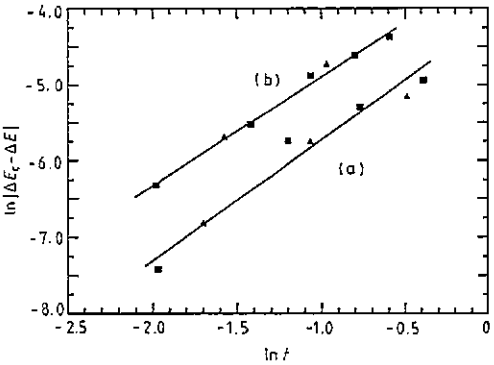

Figure 8. AgSiTe (o+c): variation of $\ln|\Delta E_c - \Delta E|$ with $\ln t$. (*a*) Orthorhombic phase; (*b*) cubic phase.

Turning to the E_0 versus T data for the cubic case, shown in figure 6, since the magnetic data indicate that $T_N = 150$ K, the values of E_0 that could be used in the fit to (7) were limited to the temperature range 225–300 K, plus the low-temperature values giving $E_{on}(0) = 1.275$ eV. Thus, in this case, Φ was taken to be 220 K, and a value of $V/2 = 3.80 \times 10^{-5}$ eV K^{-1} obtained from a plot of E_0 versus X. The resulting curve of E_{on} versus T is shown in figure 6. Values of $\Delta E(= E_0 - E_{on})$ are negative and $|\Delta E|$ has a maximum value of 14.4 meV, the curve of $|\Delta E|$ versus T being of similar shape to that shown in figure 6 for the orthorhombic case, with the maximum occurring at $T = 145$ K. Thus, as in the orthorhombic case, this was taken to be the value for T_N in the graph of $\ln|\Delta E_c - \Delta E|$ versus $\ln t$ shown in figure 8. Again a good straight line is obtained, which gives values of $\mu = -0.52$ and $P = -51$ meV.

3.3. CuSiSe (o)

The previous crystallographic work [10] showed that CuSiSe occurs only with the orthorhombic structure and the magnetic susceptibility results [11] show it to be

antiferromagnetic with a T_N value of 10 K. The variation of $\ln(I_0/I)$ with $h\nu$ obtained at 300 K in this case is shown in figure 9. This curve shows a different form from those considered above, and when a graph of $(\alpha h\nu)^2$ was plotted, it showed appreciable curvature. However, it was found that a graph of $(\alpha h\nu)^{1/2}$ was a good straight line as shown in figure 9, indicating that the initial absorption could be due to an indirect gap, i.e. that the lowest-energy gap in this case could possibly be indirect with a value of 2.030 eV. An alternative possibility is that this initial absorption is due to internal Mn transitions which have been observed with $II_{1-z}Mn_zVI$ alloys etc (see e.g., [14]). Whatever the cause of the initial absorption, it is seen in figure 9 that at $h\nu = 2.29$ eV, the graph shows a relatively sudden increase above the linear form. This is typical of the behaviour observed when a direct gap occurs at an energy a little above the indirect-gap value, and it has been taken as a direct gap in this case. Since only one structure is observed for CuSiSe, it appears that the observed direct gap belongs to this structure. Very few points in the $\ln(I_0/I)$ versus $h\nu$ curve could be observed for the direct-gap case, because of the high absorption of the sample caused by the relatively large thickness. It was not possible to produce a sample that was appreciably thinner, because these polycrystalline samples tend to crumble during polishing. Thus the value of the direct gap could not be obtained by the usual extrapolation method, and so the value was taken to be the point on the $(\alpha h\nu)^{1/2}$ graph at which the effect of the direct gap could be first observed. As a result, the direct gap E_0 value is quoted only to ± 0.01 eV.

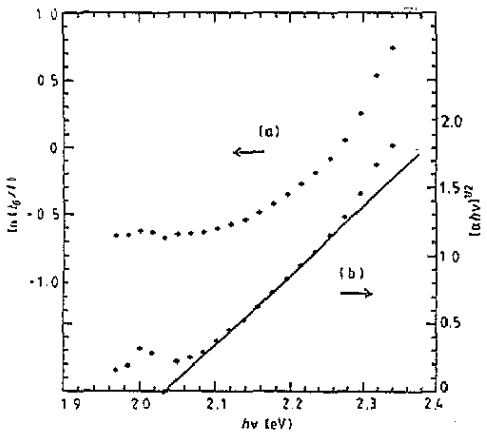

Figure 9. CuSiSe (o): variation of (*a*) $\ln(I_0/I)$ and (*b*) $(\alpha h\nu)^{1/2}$ with photon energy $h\nu$.

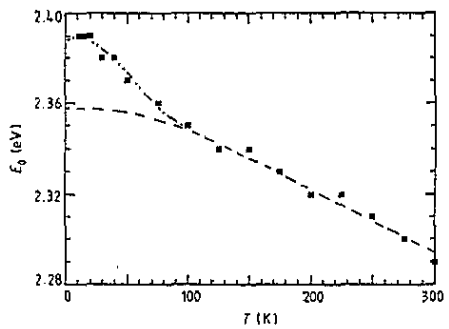

Figure 10. CuSiSe (o): variation of optical energy gap E_0 with temperature T. ■, experimental values; – – –, E_{on} values from fit to Manoogian–Leclerc equation; — · · —, E_0 values given by $E_{on} + \Delta E$.

Measurements at a range of different temperatures gave very similar results to those described above, and values of the two energy gaps were determined at each temperature. The lower gap varied very little with temperature, all the values found lying in the range 2.03–2.05 eV, and these will not be considered further here. Values of the direct gap E_0 were determined in each case to ± 0.01 eV as indicated above, and the variation of E_0 with temperature is shown in figure 10. The curve is very similar in shape to that for CuGeS (o) shown in figure 2, as is to be expected from the magnetic data. Again, it was assumed that $\Phi = 220$ K, and E_0 values in the temperature range 100–300 K fitted to (5),

using the graphical method shown in figures 3 and 7, and slope and intercept values gave $V/2 = 7.44 \times 10^{-5}$ eV K^{-1} and $E_{on}(0) = 2.358$ eV. The resultant curve of E_{on} versus T is shown in figure 10. With the experimental uncertainty of ± 0.01 in E_0, the values of ΔE were not sufficiently accurate to allow the $\ln|\Delta E_c - \Delta E|$ plot as used above. However, in all of the above cases, μ was found to be close to -0.5. Hence values of ΔE were calculated in this case from (6), taking $\mu = -0.5$ and using various values of P, as was done previously in the case of AgGeSe (o) [16]. A value of $P = 2.9$ meV was found to give a good fit to the experimental data as is shown in figure 10.

3.4. AgGeSe (o)

The previous crystallographic [10] and magnetic [11] results show that AgGeSe has only the orthorhombic structure and that this phase is ferrimagnetic with a T_N value of 64 K. Measurements of E_0 versus T were made previously [16] and the results analysed as described above, but using a value of $\mu = 0$ as proposed by Kasuya and Kondo [20]. Here, the analysis has been repeated with the value of μ taken as -0.5, in line with the values obtained above. The variation of E_0 with T is shown in figure 11. The data in the range 150–300 K were fitted to (5), assuming again that $\Phi = 220$ K. Values of ΔE were determined for various values of P, and the calculated values of E_0 as a function of T for the case when $P = -4.5$ meV are shown in figure 11, where it is seen that the fitted values agree well with the experimental data.

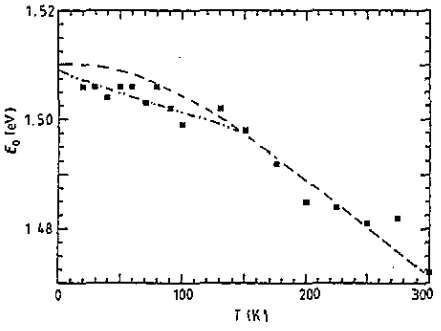

Figure 11. AgGeSe (o): variation of optical energy gap E_0 with temperature T. ■, experimental values; – – –, E_{on} values from fit to Manoogian–Leclerc equation; — · · —, E_0 values given by $E_{on} + \Delta E$.

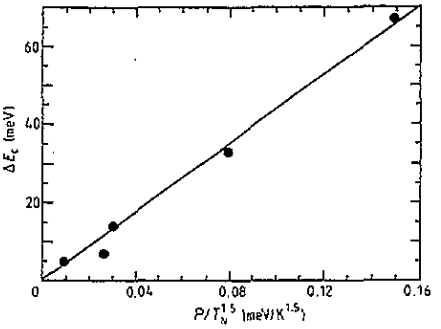

Figure 12. Variation of maximum magnetic contribution ΔE_c with $P/T_M^{1/5}$ for all phases investigated.

4. Discussion

Values of optical energy gap E_0 have been obtained for three ferrimagnetic and two antiferromagnetic phases of $I_2.Mn.IV.VI_4$ compounds, and in all cases the magnetic effects on the energy gap around the critical temperature T_N are in good agreement with the predictions of Alexander *et al* [12]. Thus, in the ferrimagnetic cases, the magnetic contribution ΔE to the band gap is negative, and in the cases of AgSiTe (o) and AgSiTe (c) the values of ΔE show a symmetrical variation, peaking at T_N. For the

two antiferromagnetic samples, ΔE is positive and has a maximum at T_N as predicted by Alexander *et al*. For three cases, the values of ΔE were used to plot lines of $\ln|\Delta E_c - \Delta E|$ versus $\ln t$, and reasonable straight lines were obtained, which gave values of the exponent μ close to -0.5 in all three cases. For the other two cases, a value of $\mu = -0.5$ and a fitted value of P gave values of E_0 in good agreement with the experimental data. For the critical region around T_N, where short-range spins dominate, Kasuya and Kondo [20] indicated that μ should have a value close to zero, while for the non-critical region, Alexander *et al* indicated that μ should have a value of +0.5. The results for the semimagnetic semiconductor spin-glass alloys such as $Cd_xZn_yMn_zTe$ [14, 15] showed good agreement with these predictions. However, for the present materials, all of the present results indicate a value of μ close to -0.5. As indicated in the magnetic work [11], the dominant exchange interaction mechanisms in the present compounds may be different from those for the semimagnetic semiconductor alloys, which could possibly explain the difference in the values of μ in the two cases.

In addition to the values of T_N and μ, values for P and ΔE_c were obtained for each case, and it is of interest to compare these values obtained for the different phases. The curve of ΔE versus T, as shown in figure 6, is symmetrical about T_N, and if $T_N + \Delta T$ is defined as the temperature at which ΔE becomes negligible, then ΔT gives a measure of the width of the ΔE curve. Values of the parameters T_N, μ, P, ΔE_c and ΔT for the five phases investigated are given in table 1. The values of T_N and μ have been discussed in the magnetic work [11] or above, but the values of the other parameters can be considered here. As indicated in previous optical work [14], P is a measure of the strength of the total spin interaction on the band-gap variation, and for the spin-glass $Cd_xZn_yMn_zTe$ alloys, in which the cations are randomly distributed, P varies linearly with z above the percolation limit and has a value of approximately 2 meV at $z = 0.25$, the Mn concentration equivalent to that of the present materials. In these, the Mn atoms are ordered, probably with different ordered structures occurring in different phases [10]. For the antiferromagnetic cases (CuGeS (o) and CuSiSe (o)), the values of P are of the same order of magnitude as for the spin-glass alloys, which also, of course, have antiferromagnetic exchange. The ferrimagnetic samples, however, show a wider range of P values, AgGeSe (o) having a magnitude similar to that for the antiferromagnetic cases, but AgSiTe (o) and AgSiTe (c) having P values approximately ten times larger than in the antiferromagnetic cases. Although the detailed magnetic structure of these ferrimagnetic materials is not as yet known, both ferromagnetic and antiferromagnetic exchanges can be expected to be present and to counteract each other in determining P. Thus, the larger values of P observed can probably be attributed to the dominance of the ferromagnetic effects, which correlates with the higher values of T_N observed for these cases.

Table 1. Parameter values determined from analysis—assumed values in parentheses.

	μ	P (meV)	ΔE (meV)	T_N (K)	ΔT (K)
CuGeS (o)	−0.55	4.7	67	10	92
CuSiSe (o)	(−0.5)	2.5	33	10	80
AgSiTe (o)	−0.52	−23	7.0	93	80
AgSiTe (c)	−0.52	−53	14.4	145	82
AgGeSe (o)	(−0.5)	−4.5	4.5	64	76

Turning to the other parameters in table 1, interesting experimental results are that the values of ΔE_c are largest for the antiferromagnetics, which have small P values, and that,

within the limits of experimental error, the values of ΔT are constant at about 80–90 K, independent of the values of T_N and P. At the temperature $T_N + \Delta T$, (3) takes the form

$$\Delta E_c = (P/T_N^{1.5})(\Delta T^{1.5}/1.5) \tag{8}$$

so that with ΔT constant, ΔE_c is proportional to $P/T_N^{1.5}$. Using the experimental values in table 1, figure 12 shows a plot of ΔE_c versus $P/T_N^{1.5}$. This is seen to be linear through the origin with a slope agreeing within 10% with that indicated by (8). Thus it is seen that the equation of Alexander *et al* fits not only the data for each separate case, but the combined results for the different phases. The linear behaviour in figure 12 depends upon the experimentally observed fact that ΔT is constant, independent of the phase investigated. Study of the data presented previously [14, 15] for the $Cd_xZn_yMn_zTe$ and $Cd_{1-z}Mn_zTe_{1-y}Se_y$ alloy systems indicates that similar results apply in those cases also, with the values of ΔT again being approximately 80 K. The values of ΔT given here are the experimental ones, i.e. the constancy of ΔT is purely empirical. There appears to be no indication in the analysis of Alexander *et al* as to why ΔT has the same constant value for these various cases, and further theoretical consideration appears to be needed.

A different approach to the analysis of magnetic effects on the value of the optical energy gap has been used by various authors [21–23]. In a simple model, the magnetic contribution to the energy gap is taken to be proportional to the product of the temperature and the magnetic susceptibility χ. This method was used for spin-glass semimagnetic semiconductors such as $Cd_{1-z}Mn_zTe$, which have antiferromagnetic exchange interaction and which show E_0 versus T behaviour similar to that presented in figure 2, assuming that the contribution proportional to χT caused a reduction in the band gap. Thus an approximate fit to the E_0 versus T curves was obtained. However, this simple model cannot be used for the ferrimagnetic types of E_0 versus T curve shown in figures 6 and 11. Thus at this stage of analysis, all of the magnetic effects observed in the present work can be fitted by the analysis of Alexander *et al* but not by that of Rys *et al* [24].

5. Conclusions

The magnetic contributions to the optical energy gap in the temperature range around the critical point T_N have been determined for four orthorhombic phases and one cubic phase belonging to the $I_2.Mn.IV.VI_4$ type of compound. In this work, the variation of the optical energy gap with temperature has been obtained from optical absorption measurements and the values of the gap E_{on} to be expected in the absence of magnetic effects determined by extrapolation from higher-temperature values using the Manoogian–Leclerc equation [18]. In all cases, the data could be fitted well by the theoretical analysis of Alexander *et al*. However, the value of the critical exponent determined from analysis of the experimental data was in these cases -0.5, as opposed to the values of zero in the critical range and $+0.5$ in the non-critical range proposed theoretically [12, 20] and observed for a range of spin-glass $II_{1-z}Mn_zVI$ alloys [14, 15]. Overall, the analysis of Alexander *et al* appears to give a very good description of the experimental data.

References

[1] Furdyna J K and Kossut J 1989 *Diluted Magnetic Semiconductors, Semiconductors and Semimetals* (New York: Academic) ch 1

[2] Wolff P A, Heimann D, Isaacs E D, Becla P, Foner S, Ram-Mohan L R, Ridgley D H, Dwight K and Wold D 1987 *High Magnetic Fields in Semiconductor Physics* ed G Landwehr (Berlin: Springer)
[3] Wolff P A and Ram-Mohan L R 1989 *Diluted Magnetic (Semimagnetic) Semiconductors* vol 89, ed R L Aggarwal, J K Furdyna and S von Molnar (Pittsburgh, PA: Materials Research Society) p 1
[4] Shapira Y, McNiff E J Jr, Oliveira H F Jr, Honig E D, Dwight K and Wold A 1988 *Phys. Rev.* B **37** 411
[5] Nitsche R, Sargent D F and Wild P 1967 *J. Cryst. Growth* **1** 52
[6] Parthé E, Yvon K and Deitch R H 1969 *Acta Crystallogr.* B **25** 1164
[7] Allemand J and Wintenberg M 1970 *Bull. Soc. Fr. Minéral Cristallogr.* **93** 14
[8] Schafer W and Nitsche R 1974 *Mater. Res. Bull.* **9** 645
[9] Guen L and Glaunsinger W S 1980 *J. Solid State Chem.* **35** 10
[10] Lamarche A-M, Willsher A, Chen X L, Lamarche G and Woolley J C 1991 *J. Solid State Chem.* **94** 635
[11] Chen X L, Lamarche A-M, Lamarche G and Woolley J C 1992 *J. Magn. Magn. Mater.* **118**
[12] Alexander S, Helman J S and Balberg J 1976 *Phys. Rev.* B **13** 304
[13] Quintero M, Marks B D and Woolley J C 1989 *J. Appl. Phys.* **66** 2402
[14] Donofrio T, Lamarche G and Woolley J C 1985 *J. Appl. Phys.* **57** 1932
[15] Chehab S F and Woolley J C 1987 *Phys. Status Solidi* b **139** 213
[16] Quintero M, Willsher A and Woolley J C 1990 *J. Magn. Magn. Mater.* **89** 185
[17] Goodchild R G, Hughes O H, Lopez-Rivera S A and Woolley J C 1979 *Can. J. Phys.* **60** 1096
[18] Manoogian A and Leclerc A 1979 *Phys. Status Solidi* b **92** K23; 1979 *Can. J. Phys.* **57** 1766
[19] Guerrero E, Quintero M and Woolley J C 1990 *J. Phys.: Condens. Matter* **2** 6119
[20] Kasuya T and Kondo A 1974 *Solid State Commun.* **14** 249
[21] Diouri J, Lascaray J P and El Amrani M 1985 *Phys. Rev.* B **31** 7995
[22] Bylsma R B, Becker W M, Kossut J and Debska M 1986 *Phys. Rev.* B **33** 8207
[23] Gaj J A, Golnik A, Lascaray J P, Coquillat D and Desjardins-Deruelle M C 1989 *Diluted Magnetic (Semimagnetic) Semiconductors* vol 89, ed R L Aggarwal, J K Furdyna and S von Molnar (Pittsburgh, PA: Materials Research Society) p 59
[24] Rys F, Helman J S and Baltensperger W 1967 *Phys. Kondens. Mater.* **6** 105